# Temperature induced transition from hexagonal to circular pits in graphite oxidation by O2

Arnaud Delehouzé, Francis Rebillat, Patrick Weisbecker, Jean-Marc Leyssale, Jean-François Epherre, Christine Labrugère, Gérard Vignoles

# Temperature induced transition from hexagonal to circular pits in graphite oxidation by $O_2$

Cite as: Appl. Phys. Lett. **99**, 044102 (2011); https://doi.org/10.1063/1.3615801
Submitted: 04 May 2011 . Accepted: 01 July 2011 . Published Online: 29 July 2011

Arnaud Delehouzé, Francis Rebillat, Patrick Weisbecker, Jean-Marc Leyssale, Jean-Francois Epherre, Christine Labrugère, and Gérard L. Vignoles

# Temperature induced transition from hexagonal to circular pits in graphite oxidation by $O_2$

Arnaud Delehouzé,[1] Francis Rebillat,[1,a)] Patrick Weisbecker,[1] Jean-Marc Leyssale,[1] Jean-Francois Epherre,[1] Christine Labrugère,[2] and Gérard L. Vignoles[1,b)]
[1]*Laboratoire des Composites ThermoStructuraux, UMR 5801, University Bordeaux 1-CNRS-Snecma Propulsion Solide-CEA, 33600 Pessac, France*
[2]*Centre de Caractérisation des Matériaux avancés (ICMCB), CNRS UPR 9048, Pessac 33600, France*

(Received 4 May 2011; accepted 1 July 2011; published online 29 July 2011)

We report on an in-situ monitoring of graphite oxidation using a high temperature environmental scanning electron microscope. A morphological transition is clearly identified around 1040 K between hexagonal pits at low temperatures and circular pits at high temperatures, with apparently no change in the kinetic law. A kinetic Monte Carlo model allows rationalizing these findings in terms of the competitive oxidation of armchair and zig-zag edge sites and provides an estimate of the rate laws associated to these two events. Extended to three dimensions, the model also explains the "in-depth" transition between the stepwise hexagons and the hemispheres observed by atomic force microscopy. © *2011 American Institute of Physics*. [doi:10.1063/1.3615801]

Oxidation is probably the main degradation route of graphite and other carbon materials.[1–3] On a microscopic perspective, oxidation proceeds by the formation of pits on a basal plane and by edge recession.[4–7] One of the most documented situations about carbon oxidation is the case of highly oriented pyrolytic graphite (HOPG) or natural graphite (NG) in a molecular oxygen atmosphere. In their pioneering study, Thomas and Hughes[8,9] report on optical microscopy observations of oxidized NG. They show that the pits have a hexagonal shape, which they attribute to different oxidation rates for armchair and zig-zag edges. Later on, many similar studies were reported, using scanning tunneling microscopy (STM) or scanning electron microscopy (SEM), and pits of either hexagonal shape,[9] circular shape,[4,10,11] or both[12] were observed. In an attempt to correlate the pit morphology with the microscopic etching mechanism of graphene edge sites, Stevens and Beebe developed a numerical model based on the etching probability of different edge sites.[13] Their model seems to show that zig-zag edges are obtained when armchair sites have a higher etch probability than zig-zag ones and that a mixture of both kinds of edges are found when the probabilities are inverted. A strong limitation of these studies is that they all deal with post-mortem morphological observations. Moreover, none of them clearly investigates the effect of the oxidation temperature or the relative stabilities of different edge sites on the pits morphologies. In this work, we directly observe, using a high temperature environmental SEM (HT-ESEM), the lateral growth of oxidation holes in seven HOPG samples, cleaved from a unique material using a razorblade. The samples were sequentially submitted to a 140 Pa atmosphere of pure molecular oxygen at temperatures ranging from 873 to 1150 K.[14]

Figure 1 shows two SEM images of the same sample after exposure to $O_2$ at 1018 K (Figure 1(a)) and 1053 K (Figure 1(b)).[14] The pits linear growth rates extracted from the different experiments carried out in that work are gathered on the Arrhenius plot of Fig. 2. As can be seen on this figure, the results present similar activation energies yet appearing rather scattered in terms of pre-exponential factor from one sample to another, although they come from the same material. Fitting all our experimental points gives the following Arrhenius parameters: $E_a = 260 \pm 10$ kJ mol$^{-1}$; $k_0 = 2.05 \pm 0.1010^9$ $\mu$m s$^{-1}$. The rate values agree quantitatively with data obtained earlier[9,15] on spectroscopic graphite

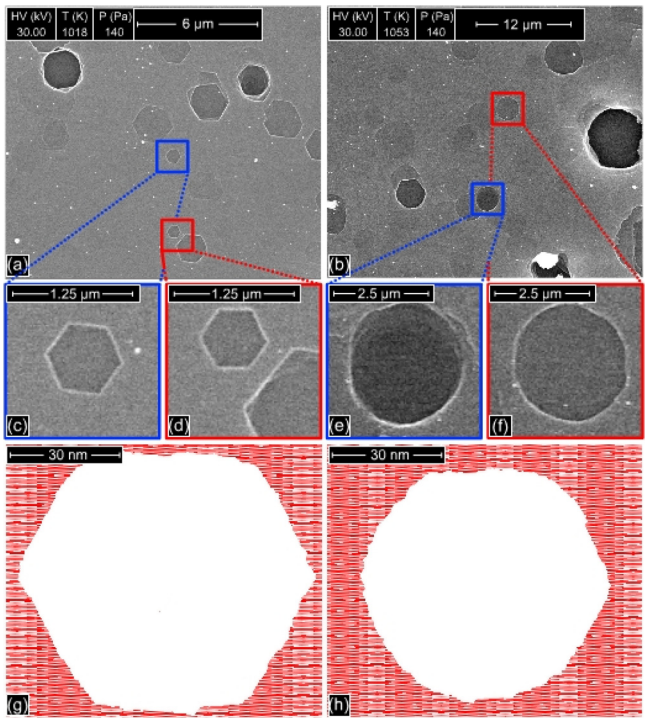


FIG. 1. (Color online) Snapshots taken from in-situ SEM observation of HOPG oxidation under a pure $O_2$ atmosphere at an operating pressure of 140 Pa at 1018 K (a) and 1053 K (b). (c)-(f): zooms on hexagonal (c) and (d) and circular (e) and (f) pits; (g) and (h): model pits obtained from KMC simulations at 1000 K (g) and 1075 K (h).

a)Electronic mail: rebillat@lcts.u-bordeaux1.fr.
b)Electronic mail: vinhola@lcts.u-bordeaux1.fr.

 

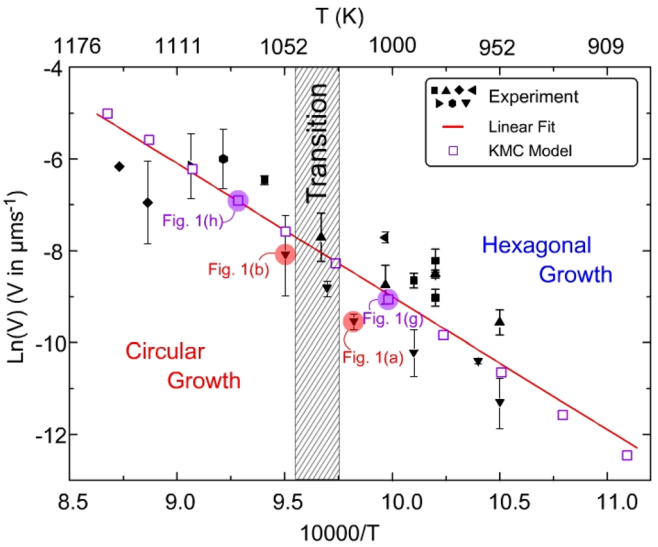


FIG. 2. (Color online) Arrhenius plot of the linear growth rate of oxidation (140 Pa of pure $O_2$) pits in HOPG showing a transition from hexagonal to circular holes. Error bars shown on the experimental rates are taken as twice the standard deviation of the rates measured on different pits (from 15 to 30) of the same sample.

from post mortem observations. The activation energy matches previous measurements[4,9] as well as density functional theory (DFT) calculations.[16] All our samples revealed only circular pits when the exposure temperature reaches 1050 K; well defined hexagons were only observed for temperatures lower than 1025 K and a mixture of poorly defined circles and hexagons is found in the window between these two temperatures. In order to investigate the effect of the pressure on the pits morphology, we performed oxidation tests in a thermal gravimetric analysis (TGA) set up at atmospheric total pressure with $O_2$ partial pressures ranging from 1 to 20 kPa (i.e., from 7 to 140 times higher than our in-situ experiments). Post mortem observations of the pits revealed exactly the same hexagon/circle transition in the same temperature range than previously observed at lower pressure in the HT-ESEM. Our results contradict past papers reporting on hexagons formed at high temperatures[9] or circles formed at low temperatures.[4,10,12]

The evolution of the pit morphology with temperature without any apparent change in the kinetic law observed on Fig. 2 is rather surprising at first sight. As postulated in previous works,[13,17] the pit morphology probably results from a competition of oxidation mechanisms on different edge sites. Indeed, looking at Figs. 1(a) and 1(d), we see that neighboring hexagons have the same orientations, indicating that the low temperature lateral growth rate is related to the graphite crystallography. Kinetic Monte Carlo (KMC)[18] is a well established technique to relate macroscopic observations to microscopic elementary kinetic mechanism and has recently been applied to the rearrangements of graphene edges in an electron microscope[19] or to the sublimation of graphene edges.[20] To rationalize our findings, we developed a KMC model of pit edge oxidation, similar to the one of Huang *et al.*,[20] in which kinetic parameters were obtained for both armchair and zig-zag edge sites (based on the temperature dependence of the pit growth kinetics and on the reproduction of the experimental pit morphology), other possible sites, much less stable, being assigned an infinite etching rate.[14] The model parameters (etching rate Arrhenius laws for armchair sites: $E_a = 234$ kj mol$^{-1}$ and $k_0 = 2.510^8$ $\mu$m s$^{-1}$ and zig-zag sites: $E_a = 284$ kJ mol$^{-1}$ and $k_0 = 6.510^9$ $\mu$m s$^{-1}$) have been adjusted to reproduce both the experimental etch rates and the morphological transition, as can be seen on Figs. 1 and 2.[14] In the low temperature domain, we have identified that armchair sites are much more reactive than zig-zag ones: this leads to hexagons with a predominance of zig-zag sites on the edges, as stated in former works.[13,16] Actually, in agreement with Stevens and Beebe,[13] we have verified that a higher etching rate for zigzag edges than for armchair edges does not lead to hexagonal pits exhibiting armchair edges, but to extremely corrugated, quasi fractal shapes, not observed experimentally by ourselves. In the high temperature domain, zig-zag and armchair etching rates are comparable, yielding circular shapes. We have carefully verified that the KMC simulations had reached a steady state in terms of the lateral growth rate (even though the diameters of the model pits are one to two orders of magnitude smaller than those observed experimentally). This is actually related to the convergence with time (or with pit radius) of the ratio of zig-zag and armchair edge site densities. Indeed, at low temperatures and for rather small pits, armchair sites react successively until a fully zig-zag edge structure is formed and eventually produces some new armchair site. The initial situation is thus binary: either an armchair site exists or not. Later on, as soon as the number of edge sites is large enough, the zig-zag/armchair edges ratio may stabilize, thus establishing a macroscopic edge roughness, and the pit growth rate becomes steady. We found out that this convergence is achieved for pits of around 2-3 nm in the hexagonal domain. Of course, it is immediately steady whatever the size in the circular pits domain.

Fig. 3 shows AFM images of a hexagonal (a) and a circular (b) oxidation pits. As can be seen, not only the lateral shape but also the in-depth profile differs when going from low to high temperature oxidation. Indeed, low temperature pits form nested hexagons with sharp steps while pits with a smooth cup shape are observed at high temperature. Actually, a profile analysis of these pits gives steps of around 3-6 nm height (i.e., 8-16 graphene sheets) for the hexagonal pit whereas we were not able to detect any steps on the circular pits. There is no straightforward explanation to the existence of those steps but we can hypothesize that they are related to defects in the material. For instance, we could think that a graphene sheet in a perfect crystallographic arrangement with an upper pitted sheet is almost instantaneously attacked by oxygen while the attack can be delayed if

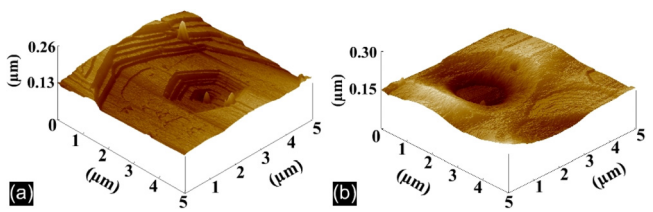


FIG. 3. (Color online) Tapping mode atomic force microscopy imaging of HOPG samples oxidized at 987 K (a) and 1037 K (b) (140 Pa of pure $O_2$).

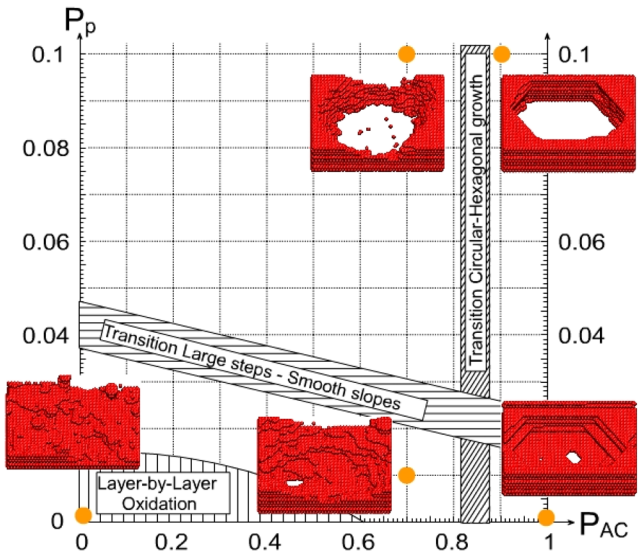


FIG. 4. (Color online) Three-dimensional kinetic Monte Carlo oxidation model. Typical pit morphologies are displayed as a function of the armchair etching ($P_{AC}$) and in-depth pitting ($P_P$) normalized probabilities ($P_{AC} + P_{ZZ} + P_P = 1$).

the sheets are a bit more distant from each other due to a turbostratic arrangement or stacking faults. Preliminary TEM observations seem to confirm this hypothesis. Nevertheless, our observations show that the in-depth propagation of the pits is much more rapid than the creation of new pits on the upper basal plane, which indicates that the presence of oxygen groups on the edge of a pitted sheet considerably accelerates the attack of the sheet directly underneath it.

Based on these observations, we have extended our KMC model to a multi-layer single pit recession model. As experimental kinetic data on the in-depth oxidation rate cannot be obtained, we simply discuss the model in terms of the relative etching probabilities of an armchair edge ($P_{AC}$), of a zig-zag edge ($P_{ZZ}$) and of an atom situated under (actually in the vicinity of) an edge of an already pitted sheet ($P_P$). At a given temperature, these probabilities are directly linked to the relative etching rates of these different varieties of carbon sites. Fig. 4 qualitatively summarizes the effects of these probabilities on the pit morphologies. As can be seen on this figure, hexagonal pits are formed when $P_{AC}$ is large compared to $P_{ZZ}$ ($P_{AC} > 0.8$) and circular ones otherwise. Obviously, the pitting probability $P_P$ has an effect on the slope of the in-depth profile and the larger $P_P$, the higher the slope. Looking at Fig. 4, some typical situations can be identified: (1) hexagonal pits with large steps ($P_{AC} \geq 0.85$, $P_P \geq 0.05$); (2) circular pits with large steps ($P_{AC} \leq 0.8$, $P_P \geq 0.05$); (3) hexagonal pits with smooth slopes ($P_{AC} \geq 0.85$, $P_P \leq 0.001$); (4) circular pits with smooth slopes ($P_{AC} \leq 0.8$, $P_P \leq 0.01$); and finally (5) a layer by layer oxidation with ill-defined shape (low values of $P_{AC}$ and $P_P$). The latter case is typical of the mono-layer oxidation with low values of the $P_{AC}/P_{ZZ}$ ratio. It leads to a spherical hole with an important edge roughness (increasing when this ratio decreases). Looking back at Fig. 3, our experimental observations correspond to situations (1) (large steps hexagons, corresponding to one large step of Fig. 3(a)) and (4) (smooth slope circles, corresponding to Fig. 3(b)).

In this work, we have shown that the oxidation of HOPG in a dry molecular oxygen atmosphere leads to hexagonal pits at low temperature and circular pits at high temperature. This transition, occurring in a narrow temperature window between 1025 and 1050 K, has been observed both at low (observed in situ in a HT-ESEM setup) and high (observed post mortem after oxidation in a TGA device) oxygen pressures. A KMC model, based on the experimental results, has allowed us to directly link this morphological transition to the competition between etching of armchair and zig-zag edge sites. Finally, AFM imaging of pits formed at low and high temperatures have respectively revealed stepwise (hexagons) and smooth (circles) in-depth patterns. This was also rationalized using 3D KMC modeling. If the models used in this work were of a purely interpretative nature, a possible and natural extension to a predictive model would be to feed it with individual etching rates of all the many possible elementary chemical etching mechanisms obtained for instance from *ab initio* calculations.[5–7]

This work has been supported by a Ph.D. Grant to A.D. by CEA and CNRS.

[1]J. Lahaye, J. Dentzer, P. Soulard, and P. Ehrburger, Carbon Gasification: The Active Site Concept, in *Fundamental Issues in Control of Carbon Gasification Reactivity* (Kluwer Academic, Dordrecht, the Netherlands, 1991).
[2]J. Rodríguez-Mirasol, P. Thrower, and L. R. Radovic, Carbon **31**, 789 (1993).
[3]J. Rodríguez-Mirasol, P. Thrower, and L. R. Radovic, Carbon **33**, 545 (1995).
[4]R. T. Yang, Chem. Phys. Carbon **19**, 163 (1984).
[5]J.-L. Li, K. Kudin, M. McAllister, R. Prud'homme, I. Aksay, and R. Car, Phys. Rev. Lett. **96**, 176101 (2006).
[6]L. Radovic, J. Am. Chem. Soc. **131**, 17166 (2009).
[7]J. M. Carlsson, F. Hanke, S. Linic, and M. Scheffler, Phys. Rev. Lett. **102**, 166104 (2009).
[8]E. E. G. Hughes and J. M. Thomas, Nature **193**, 838 (1962).
[9]J. M. Thomas and E. E. G. Hughes, Carbon **1**, 209 (1964).
[10]F. Stevens, L. Kolodny, and T. P. Beebe, Jr., J. Phys. Chem. B **102**, 10799 (1998).
[11]J. Hahn, Carbon **43**, 1506 (2005).
[12]X. Chu and L. Schmidt, Carbon **29**, 1251 (1991).
[13]F. Stevens and T. P. Beebe, Jr., Comput. Chem. **23**, 175 (1999).
[14]See supplementary material at http://dx.doi.org/10.1063/1.3615801 for more experimental details on the samples preparation and characterization; the full oxidation movies, respectively, videos M1 and M2, from which Figs 1(a) to 1(f) are taken; a description of the KMC model; and the simulated oxidation movies, respectively, videos M3 and M4, from which Figs. 1(g) and 1(h) are taken.
[15]R. J. Tyler, H. J. Wouterlood, and M. F. R. Mulcahy, Carbon **14**, 271 (1976).
[16]N. Chen and R. T. Yang, J. Phys. Chem. A **102**, 6348 (1998).
[17]E. F. Brown, Comput. Chem. **12**, 27 (1988).
[18]A. B. Bortz, M. H. Kalos, and J. L. Lebowitz, J. Comput. Phys. **17**, 10 (1975).
[19]C. Ö. Girit, J. Meyer, R. Erni, M. Rossell, C. Kisielowski, L. Yang, C.-H. Park, M. Crommie, M. Cohen, S. Louie, and A. Zettl, Science **323**, 1705 (2009).
[20]J. Y. Huang, F. Ding, B. I. Yakobson, P. Lu, L. Qi, and J. Li, Proc. Natl. Acad. Sci. **106**, 10103 (2009).